

# Pharmacokinetics and Pharmacodynamics of a Human Monoclonal Anti-FGF23 Antibody (KRN23) in the First Multiple Ascending-Dose Trial Treating Adults With X-Linked Hypophosphatemia

The Journal of Clinical Pharmacology  
 2016, 56(2) 176–185  
 © 2015 The Authors. *The Journal of Clinical Pharmacology* Published by Wiley Periodicals, Inc. on behalf of American College of Clinical Pharmacology  
 DOI: 10.1002/jcph.570

Xiaoping Zhang, PhD<sup>1</sup>, Erik A. Imel, MD<sup>2</sup>, Mary D. Ruppe, MD<sup>3</sup>, Thomas J. Weber, MD<sup>4</sup>, Mark A. Klausner, MD<sup>1</sup>, Takahiro Ito, MSc<sup>1</sup>, Maria Vergeire, MD<sup>1</sup>, Jeffrey Humphrey, MD<sup>1</sup>, Francis H. Glorieux, MD, PhD<sup>5</sup>, Anthony A. Portale, MD<sup>6</sup>, Karl Insogna, MD<sup>7</sup>, Thomas O. Carpenter, MD<sup>7</sup>, and Munro Peacock, MD<sup>2</sup>

## Abstract

In X-linked hypophosphatemia (XLH), serum fibroblast growth factor 23 (FGF23) is increased and results in reduced renal maximum threshold for phosphate reabsorption (TmP), reduced serum inorganic phosphorus (Pi), and inappropriately low normal serum 1,25 dihydroxyvitamin D (1,25[OH]<sub>2</sub>D) concentration, with subsequent development of rickets or osteomalacia. KRN23 is a recombinant human IgG1 monoclonal antibody that binds to FGF23 and blocks its activity. Up to 4 doses of KRN23 were administered subcutaneously every 28 days to 28 adults with XLH. Mean ± standard deviation KRN23 doses administered were 0.05, 0.10 ± 0.01, 0.28 ± 0.06, and 0.48 ± 0.16 mg/kg. The mean time to reach maximum serum KRN23 levels was 7.0 to 8.5 days. The mean KRN23 half-life was 16.4 days. The mean area under the concentration–time curve (AUC<sub>n</sub>) for each dosing interval increased proportionally with increases in KRN23 dose. The mean intersubject variability in AUC<sub>n</sub> ranged from 30% to 37%. The area under the effect concentration–time curve (AUEC<sub>n</sub>) for change from baseline in TmP per glomerular filtration rate, serum Pi, 1,25(OH)<sub>2</sub>D, and bone markers for each dosing interval increased linearly with increases in KRN23 AUC<sub>n</sub>. Linear correlation between serum KRN23 concentrations and increase in serum Pi support KRN23 dose adjustments based on predose serum Pi concentration.

## Keywords

X-linked hypophosphatemia (XLH), fibroblast growth factor 23 (FGF23), human anti-FGF23 antibody (KRN23), serum phosphorus, pharmacokinetics

Loss-of-function mutations in *PHEX* cause X-linked hypophosphatemia (XLH), the most common heritable form of rickets and osteomalacia. A consequence of the *PHEX* mutation is increased expression of FGF23 in bone.<sup>1,2</sup> FGF23 is a hormone that reduces the abundance of sodium-phosphate cotransporters in the apical membrane of renal proximal tubular cells, resulting in reduced renal tubular phosphate reabsorption (TmP) and serum phosphorus concentration (measured as inorganic phosphorus, Pi).<sup>3–5</sup> FGF23 also decreases renal 1 $\alpha$ -hydroxylase activity, resulting in reduced blood levels of 1,25-dihydroxyvitamin D (1,25[OH]<sub>2</sub>D). Thus hypophosphatemia and inappropriately low normal serum 1,25(OH)<sub>2</sub>D levels for the level of serum Pi represent 2 characteristic biochemical consequences of increased FGF23 observed in XLH.<sup>6,7</sup>

In children with XLH, impaired bone mineralization results in clinical and radiographic features of rickets, including lower-extremity bowing, widening of growth plates, and short stature.<sup>7,8</sup> In adults, impaired mineralization results in osteomalacia and pseudofractures.<sup>8</sup> The presence

<sup>1</sup>Kyowa Hakko Kirin Pharma Inc., Princeton, NJ, USA

<sup>2</sup>Indiana University School of Medicine, Indianapolis, IN, USA

<sup>3</sup>The Methodist Hospital, Houston, TX, USA

<sup>4</sup>Duke University Medical Center, Durham, NC, USA

<sup>5</sup>Shriners Hospital for Children, Montreal, Quebec, Canada

<sup>6</sup>University of California, San Francisco, CA, USA

<sup>7</sup>Yale Center for X-Linked Hypophosphatemia, Yale University School of Medicine, New Haven, CT, USA

This is an open access article under the terms of the Creative Commons Attribution-NonCommercial-NoDerivs License, which permits use and distribution in any medium, provided the original work is properly cited, the use is non-commercial and no modifications or adaptations are made.

Submitted for publication 29 March 2015; accepted 9 June 2015.

## Corresponding Author:

Xiaoping Zhang, PhD, Kyowa Hakko Kirin Pharma Inc., 212 Carnegie Center, Suite 101, Princeton, NJ 08540 Email: [azhang@kyowa-kirin-pharma.com](mailto:azhang@kyowa-kirin-pharma.com)

Clinicaltrials.gov identifier: NCT01340482

of a reduced mineralization rate in active osteomalacia results in increased serum and urine concentrations of biochemical markers of bone turnover.<sup>9</sup> Current therapy, typically with oral calcitriol and phosphate supplements, targets the biochemical consequences of FGF23 excess and improves bone mineralization,<sup>10,11</sup> but the underlying defect in renal Pi reabsorption is not corrected, and clinical responses in bone are highly variable among patients. Current treatment requires multiple daily doses of medication and has serious potential complications including hypercalciuria, hypercalcemia, nephrocalcinosis, nephrolithiasis, and parathyroid hyperplasia.<sup>12,13</sup> Thus, safer and more efficacious therapies are needed.<sup>14</sup>

KRN23 is a recombinant human immunoglobulin (Ig) G<sub>1</sub> monoclonal antibody that binds intact FGF23 (and FGF23 fragments) at the N-terminal domain. An antimurine FGF23 antibody binding to FGF23 blocked biologic activity of FGF23 in mice.<sup>12</sup> In hypophosphatemic Phex-deficient mice, injection of antibody to murine FGF23 increased both serum Pi and 1,25(OH)<sub>2</sub>D concentrations by increasing renal expression of type IIa sodium-phosphate cotransporters and renal 1 $\alpha$ -hydroxylase activity, respectively.<sup>15</sup> After serial injections in these mice, defective mineralization, abnormal cartilage development, and delayed skeletal growth were improved, confirming that increased FGF23 underlies the murine metabolic bone disease and suggests that inhibition of FGF23 activity may be useful for treating rickets and osteomalacia in humans with XLH.

Recently, a phase 1 randomized, placebo-controlled, double-blind trial of KRN23 in adults with XLH demonstrated that a single intravenous or subcutaneous dose of KRN23 resulted in prolonged inhibition of FGF23 activity.<sup>16,17</sup> Serum Pi, TmP per glomerular filtrate rate (TmP/GFR), and serum 1,25(OH)<sub>2</sub>D increased in a dose-dependent manner, and the half-life of KRN23 given subcutaneously was 13 to 19 days. The greater than 4-week duration of the Pi effect suggested that subcutaneous injection of KRN23 every 4 weeks might be an effective treatment to increase serum Pi in XLH patients. Subsequently a phase 1/2 dose-escalation study of repeated subcutaneous doses of KRN23 at 28-day intervals in adults with XLH was undertaken to assess the efficacy and safety of KRN23.<sup>18</sup> We report here the secondary objective of the study, which was to evaluate the pharmacokinetics (PK), pharmacodynamics (PD), and PK/PD relationships of serum KRN23 and the biochemical variables.

## Methods

### Subjects

The study was approved by the relevant local institutional review boards (IRBs): Human Research Protection Program, at Yale University School of Medicine; Human Subjects Office at Indiana University IRB; Copernicus Group IRB at

Research Triangle Park in North Carolina; Committee for the Protection of Human Subjects at the University of Texas Health Science Center Houston; Committee on Human Research at the University of California San Francisco; and IRB at McGill University. The study was conducted in accordance with the International Conference on Harmonization E6 Good Clinical Practice guidelines and the Declaration of Helsinki. All subjects provided written informed consent prior to screening. Adults ( $\geq 18$  years of age) with a clinical diagnosis of XLH, intact serum FGF23  $\geq 30$  pg/mL,<sup>19</sup> TmP/GFR  $< 2.0$  mg/dL, creatinine clearance  $\geq 60$  mL/min (Cockcroft-Gault equation), and serum calcium  $< 10.8$  mg/dL at screening were eligible. Key exclusion criteria were pregnancy or lactation; history within 3 months before screening of major surgery, or receipt of a monoclonal antibody or a live (attenuated) vaccine. Vitamin D or vitamin D analogues, calcium or phosphate supplements, or aluminum hydroxide were not permitted for at least 10 days before screening and throughout the study.

### Study Design and Treatment

The dose of KRN23 was calculated using the subject's weight on the dosing day. Subjects received a subcutaneous dose of KRN23 every 28 days, for up to 4 doses, using a stepwise escalation of 0.05, 0.1, 0.3, and 0.6 mg/kg. For each subject, the dose was increased based on the fasting serum Pi concentration on day 26, as follows: if the serum Pi on day 26 was (1)  $\leq 2.5$  mg/dL, the dose increased 1 dose level; (2)  $> 2.5$  but  $\leq 3.5$  mg/dL, the previous dose was repeated; (3)  $> 3.5$  mg/dL, the dose was withheld, and Pi was retested 28 days later. If the repeat was (1)  $\leq 2.5$  mg/dL, the most recent dose was repeated; (2)  $> 2.5$  but  $\leq 3.5$  mg/dL, the dose was reduced 1 dose level; (3)  $> 3.5$  mg/dL, the dose was withheld and serum Pi reevaluated another 28 days later at the discretion of the investigator and the sponsor. Dosing could be modified based on safety observations, including adverse events and safety laboratory parameters.

### Investigational Product

KRN23 was manufactured, labeled, and packaged in single-use vials by Kyowa Hakko Kirin Co., Ltd (Tokyo, Japan).

### Pharmacokinetic Assessments

Blood samples for measurement of KRN23 concentration were obtained before each dose, on days 3, 7, 12, 18, and 26 after each dosing and on day 36 after the fourth dose or at early withdrawal. Serum KRN23 concentrations were measured at Kyowa Hakko Kirin California, Inc (La Jolla, California) using a validated sandwich enzyme-linked immunosorbant assay (ELISA; data on file), which employs an anti-KRN23 mouse monoclonal antibody as the capture antibody and a biotinylated anti-KRN23 monoclonal antibody as the detection antibody (both were supplied from Kyowa Hakko Kirin Co., Ltd, Japan).

Using a streptavidin-alkaline phosphatase conjugate to catalyze the chemiluminescent substrate, the resulting chemiluminescent light intensity was measured, and the concentrations of KRN23 were calculated. The calibration range was 50 to 3000 ng/mL. The lower limit of quantification was 50 ng/mL. The assay accuracy (relative error) and precision (coefficient of variation for the mean) were within acceptance criteria ( $< \pm 20\%$ ) for a majority of quality control samples (94.6%). A small amount of quality control samples (5.4%) showed relative errors between 20.7% and 26.7%. Ten individual lots of pooled human serum were spiked with 50 ng/mL KRN23. The relative error of detection ranged from -11.4% to 7.2%, whereas all the unspiked individual lots yielded concentrations below the low limit of quantification (50 ng/mL), confirming the selectivity of the assay.

#### Detection of Anti-KRN23 Antibodies

Serum samples for anti-KRN23 antibodies were obtained before each dose and on day 36 after the fourth dose or at early withdrawal. Samples were assayed using a validated electrochemiluminescent (ECL) method. A sequential screening algorithm employed an initial screening assay, a subsequent immunodepletion assay, and a neutralizing assay at Kyowa Hakko Kirin California, Inc (La Jolla, California). Testing only proceeded to the subsequent assay step if the earlier assay result was positive.

The bridging ECL format for both the screening and specificity confirmation assays begins with a streptavidin-coated plate supplied by Meso Scale Discovery (MSD). In the screening assay, control and bioanalytical samples are first diluted with diluent buffer on a 96-well, round-bottom polypropylene plate. Then, diluted samples are incubated with a Master Mix containing biotinylated KRN23 (capture antibody) and ruthenylated-KRN23 (detection antibody). Following incubation with the labeled drug mixture, samples are transferred from the polypropylene plate to the blocked, streptavidin-coated MSD plate in duplicate and incubated at room temperature with shaking. After incubation, unbound material is washed away, and MSD Read Buffer (ECL substrate) is added to the wells. The ECL signal intensity is immediately read using an MSD Sector Imager measuring MSD signal counts, which is used to evaluate the presence of anti-KRN23 antibodies and assess the specificity of any antibodies relative to KRN23. The specificity confirmation assay follows the same format as the screening assay, except that prior to incubation with the labeled drug mixture, controls and bioanalytical samples are first diluted with buffer containing immunodepletive antigen (KRN23). Screening assay cut point was 1.88 for signal ratio.

#### Pharmacodynamic Assessments

Blood samples for pharmacodynamic assessments were collected at screening, before each dose, on days 3, 7, 12,

18, and 26 after each dose, and on day 36 after the last dose (final visit). Biochemical measurements included serum Pi, 1,25(OH)<sub>2</sub>D, 25-hydroxyvitamin D (25[OH]D), creatinine, calcium, and parathyroid hormone (PTH). Pi, calcium, and creatinine were measured in the corresponding 2-hour urine collected after an 8-hour fast on the day before the first injection and on days 3, 7, 12, and 26 after each injection and on day 36 after the last injection. Calcium, Pi, and creatinine were measured in a 24-hour urine collected on the day before the first injection, on days 3, 12, and 26 after each injection, and on day 36 after the last injection. TmP/GFR was calculated using an established equation based on glomerular filtration rate calculated from creatinine clearance.<sup>20</sup> Blood and urine samples for measurement of bone turnover markers were collected prior to each dose and at the final visit. Bone formation markers included serum bone alkaline phosphatase (BALP), procollagen type 1, N propeptide (PINP), and osteocalcin. Bone resorption markers included serum carboxy-terminal cross-linked telopeptide of type 1 collagen (CTx), and urine amino-terminal cross-linked telopeptide of type 1 collagen (NTx).

Serum intact FGF23 was measured at baseline using an ELISA assay (Kainos Laboratories, Japan). All other biochemical variables in serum (25[OH]D, 1,25[OH]<sub>2</sub>D, PTH, BALP, CTx, osteocalcin, Pi, calcium, and creatinine) and in urine samples (Pi, calcium, creatinine, and NTx) were analyzed by Quest Diagnostics Inc. using standardized automated methodologies.

#### Pharmacokinetic and Statistical Analysis

Pharmacokinetic (PK) parameters were estimated using serum concentration–time data for all accumulated doses from day 1 to the last follow-up visit on day 120. A noncompartmental analysis method was employed to derive PK parameters.<sup>21</sup> These included area under the serum concentration–time curve from zero to last measured concentration ( $AUC_{last}$ ), area under the serum concentration–time curve from zero to infinity ( $AUC_{inf}$ ), apparent volume of distribution ( $V/F$ ), apparent clearance ( $CL/F$ ), and terminal elimination half-life after the fourth dosing interval ( $t_{1/2}$ ). Pharmacokinetic parameters estimated for each 28-day dosing interval included area under the serum concentration–time curve ( $AUC_n$ ), maximum serum concentration ( $C_{max,n}$ ), predose serum concentration ( $C_{min,n}$ ), and time to peak serum concentration ( $T_{max,n}$ ), where  $n$  denotes the number of doses received (1, 2, 3, and 4) up to the measured dosing interval. Descriptive statistics were used for serum KRN23 concentration data and PK parameters. All PK parameters were derived using Phoenix WinNonlin (version 6.3; Pharsight Company, Mountain View, California).

Area under the effect concentration–time curve for the change from baseline prior to the first dose for TmP, serum Pi, and 1,25(OH)<sub>2</sub>D were calculated for day 1 to day 120 of

treatment or up to the last measured time before withdrawal ( $AUEC_{last}$ ) and for each of the 4 dosing intervals ( $AUEC_1$ ,  $AUEC_2$ ,  $AUEC_3$ , and  $AUEC_4$ ). Pharmacodynamic (PD) variables were estimated using SAS software (version 9; SAS Institute Inc., North Carolina).

Scatterplots were generated to explore PK/PD correlations using  $AUC_n$  for PK measures and  $AUEC_n$  for PD measures. Pearson correlation coefficients ( $R$ ) were derived from linear regression as appropriate.

During the study conduct, TmP/GFR was manually derived from a nomogram developed by Walton and Bijvoet.<sup>24</sup> In the analysis, TmP/GFR was calculated from the following equation<sup>20</sup>:

$$TmP/GFR(mg/dL) = TRP \times [serum phosphorous (mg/dL)] \text{ (if } TRP \leq 0.86); \quad (1)$$

$$TmP/GFR(mg/dL) = 0.3 \times TRP / (1 - 0.8 \times TRP) \times [serum phosphorous(mg/dL)] \text{ (if } TRP > 0.86); \quad (2)$$

where tubular reabsorption of phosphate (TRP) is  $1 - (2\text{-hour urine phosphorus [mg/dL]} / (\text{serum phosphorus [mg/dL]} \times (\text{serum creatinine [mg/dL]} / (2\text{-hour urine creatinine [mg/dL]})))$ .

The TmP/GFR values derived from the 2 methods were compared, but only the calculated results are reported.

## Results

### Demographics and Baseline Characteristics (Table 1)

KRN23 was administered to 28 subjects. Twenty-six subjects (92.9%) received 4 doses; 1 subject withdrew after 3 doses because of injection-site urticaria. One subject withdrew after 1 dose because of the presence of moderate to severe preexisting nephrocalcinosis (this subject did not provide PK samples). The number of subjects who contributed to the analysis was 27. Eighteen subjects (64%) were female, and 26 (93%) were white; mean body weight was 75.6 kg, and mean age was 41.5 years. Mean TmP/GF ( $1.6 \pm 0.4$  mg/dL) and serum Pi ( $1.9 \pm 0.3$  mg/dL) were below the normal reference range. The mean  $1,25(OH)_2D$  level ( $36.6 \pm 14.3$  pg/mL) was within the normal reference range, and only 2 subjects were decreased below the reference range. The mean  $25(OH)D$  was  $25.0 \pm 9.1$  ng/mL. Mean PTH was increased at 74 pg/mL, and mean serum FGF23 was increased at 91 pg/mL. Mean serum calcium, fasting 2-hour urine calcium/creatinine ratio, and 24-hour urine calcium excretion were in the normal range. No subject was hypercalciuric. Mean values for both formation markers (BALP, osteocalcin, PINP) and resorption markers (NTx, CTx) were in the normal reference ranges, although some subjects had increased levels.

### KRN23 Doses

All subjects received an initial dose of 0.05 mg/kg. For the second dose, 26 (96.3%) received 0.1 mg/kg, and 1 remained at 0.05 mg/kg (1 withdrew). For the third dose, 25 subjects (92.6%) received 0.3 mg/kg, 1 continued at 0.05, and 1 at 0.1 mg/kg. For the fourth dose, 16 subjects (61.5%) received 0.6 mg/kg, 8 continued at 0.3 mg/kg, 1 increased from 0.05 to 0.1 mg/kg, and 1 from 0.1 to 0.3 mg/kg (1 withdrew). No subject required dose delay or reduction. The mean total KRN23 doses administered increased from the first to the fourth dose:  $0.05 \pm 0.0$ ,  $0.10 \pm 0.01$ ,  $0.28 \pm 0.06$ , and  $0.48 \pm 0.16$  mg/kg for dosing intervals 1, 2, 3, and 4, respectively.

### Pharmacokinetic Results

The mean KRN23 PK exposure ( $AUC_n$ ) increased from  $174 \pm 63$  after the first dose to  $2610 \pm 974$   $\mu\text{g} \cdot \text{h/mL}$  after the fourth dose (Table 2). The  $AUC_{last}$  for the 4 dosing intervals was  $4340 \pm 1320$   $\mu\text{g} \cdot \text{h/mL}$ . The extrapolated part for  $AUC_{inf}$  ( $5240 \pm 1880$   $\mu\text{g} \cdot \text{h/mL}$ ) compared with  $AUC_{last}$  was less than 25%. The mean  $T_{max}$  values were similar (7.0 to 8.5 days) across the 4 dosing intervals. The terminal mean  $t_{1/2}$  estimated after the fourth dosing interval was 16.4 days. Mean serum KRN23 concentration increased as mean dose increased (Figure 1A). The mean KRN23 serum PK exposures (log-transformed  $C_{max,n}$ ,  $C_{min,n}$ , and  $AUC_n$ ) increased with increased log dose in a proportional manner, with correlation coefficients ( $R$ ) of 0.998, 0.993, and 0.998, respectively (Figure 1B shows  $AUC_n$ ). The mean intersubject variability in  $AUC_n$  ranged from 30% to 37%. The CL/F was  $0.186 \pm 0.078$  mL/h/kg, and the V/F was  $98.3 \pm 34.6$  mL/kg.

### Pharmacokinetic and Pharmacodynamic Relationships

**Serum Phosphorus.** Mean serum Pi concentrations increased to a maximum on day 7, returned to near baseline by day 28 after each dose, and increased with successive doses of KRN23 (Figure 2A).  $AUEC_n$  for serum Pi was linearly correlated with  $AUC_n$  for serum KRN23 ( $R = 0.812$ ; Figure 2B).

**TmP/GFR.** TmP/GFR values increased to a maximum on day 7 after each dose, returned to near baseline by day 28, and increased with successive doses of KRN23 (Figure 2C).  $AUEC_n$  for TmP/GFR was linearly correlated with serum KRN23  $AUC_n$  ( $R = 0.822$ ; Figure 2D).

**$1,25(OH)_2D$ .** Serum  $1,25(OH)_2D$  concentrations increased to a maximum by day 3 after each dose and then returned to near baseline values by day 28 (Figure 2E).  $AUEC_n$  for serum  $1,25(OH)_2D$  were linearly correlated with serum KRN23  $AUC_n$  ( $R = 0.666$ ; Figure 2F).

**Bone Markers.** The  $AUEC_n$  for serum bone formation markers increased as KRN23  $AUC_n$  increased with moderate correlation. The correlation coefficients ( $R$ )

**Table 1.** Subject Demographics and Disease Characteristics at Baseline

Characteristic <sup>a</sup>	KRN23	Reference Range
Demographics	n = 27	
Age (years)	41.5 ± 14.0 (19–66)	NA
Sex (male/female), n	9/18	NA
Race (white/other), n	26/1	NA
Weight (kg)	75.6 ± 19.9 (51.3–121.9)	NA
Height (cm)	150.1 ± 12.5 (121.9–170.2)	NA
Serum FGF23 (pg/mL), median (range)	91 (36–3520)	8–54 <sup>22</sup>
Serum Pi (mg/dL)	1.9 ± 0.3 (1.2–2.8)	2.5–4.5 <sup>23</sup>
TmP/GFR (mg/dL)	1.6 ± 0.4 (0.8–2.3)	2.5–4.2 <sup>24</sup>
Serum 1,25(OH) <sub>2</sub> D (pg/mL) <sup>b</sup>	36.6 ± 14.3 (10–62)	15.9–55.6 <sup>25</sup>
Serum 25(OH)D, ng/mL	25.0 ± 9.1 (12–44)	32–100 <sup>25</sup>
Serum total calcium (mg/dL)	9.1 ± 0.4 (8.5–10.2)	8.5–10.3 <sup>23</sup>
Serum PTH (pg/mL), median (range)	74 (38–143)	10–65 <sup>23</sup>
BALP (μg/L)	28.3 ± 12.8 (8.2–52.4)	M: 3.7–20.9 F: 2.9–14.5 (premenopausal) F: 3.8–22.6 (postmenopausal) <sup>23</sup> M: 22–87 (18+ years) <sup>22</sup> F: 19–83 (premenopausal) <sup>23</sup> F: 16–96 (postmenopausal) <sup>23</sup> M: 8.0–370 <sup>23</sup>
PINP (ng/mL)	64.1 ± 30.7 (11–123)	F: 7.0–38.0 (pre- and postmenopausal without osteoporosis) <sup>23</sup> M: 12–99 (18–29 years) <sup>23</sup> M: 9–60 (30–59 years) <sup>23</sup> M: not established (60+ years) <sup>23</sup> F: 4–64 (premenopausal, 18+ years) <sup>23</sup> M: 87–11200 (18–129 years) <sup>23</sup> M: 70–1780 (30–139 years) <sup>23</sup> M: 60–1700 (40–149 years) <sup>23</sup> M: 87–1345 (50–168 years) <sup>23</sup> M: not established (69+ years) <sup>23</sup> F: 64–1640 (18–129 years) <sup>23</sup> F: 60–1650 (30–139 years) <sup>23,22</sup> F: 40–1465 (40–149 years) <sup>23</sup> F: not established (50+ years) <sup>23,22</sup>
Osteocalcin (ng/mL)	29.3 ± 17.7 (6.5–95.4)	
NTx/creatinine ratio (nmol BCE/mmol)	41.8 ± 20.3 (12–112)	
CTx (pg/mL)	752 ± 389 (214, 1899)	
24-Hour urine calcium (mg/24 hours), median (range)	67 (11–253)	M: 50–1300 F: 50–1250 <sup>23</sup>
24-Hour urine creatinine (g/24 hours), median (range)	1.13 (0.54–3.01)	0.63–12.50 <sup>23</sup>
2-Hour calcium/creatinine ratio (mg/g creatinine), median (range)	36 (7–192)	M: 10–1240 <sup>23</sup> F: 10–1320 <sup>23</sup>
24-Hour urine phosphate (mg), median (range)	2244 (1087–4785)	M: 1103–14 903 <sup>23</sup> F: 521–13 677 <sup>23</sup>

<sup>a</sup>Data are presented from baseline and are expressed as mean ± standard deviation (range) except where noted.

<sup>b</sup>n = 24 for serum 1,25(OH)<sub>2</sub>D.

1,25(OH)<sub>2</sub>D, 1,25-dihydroxyvitamin D; 25(OH)D, 25-hydroxyvitamin D; BALP, bone alkaline phosphatase; F, female; FGF23, fibroblast growth factor 23; PTH, parathyroid hormone; M, male; NA, not applicable; Pi, serum phosphorus (inorganic); TmP/GFR, renal tubular maximum reabsorption rate of phosphate to glomerular filtration rate.

were 0.373 for BALP (Figure 3A), 0.484 for PINP (Figure 3B), and 0.537 for osteocalcin (Figure 3C). The AUEC<sub>n</sub> for the bone resorption markers increased as KRN23 AUC<sub>n</sub> increased. The moderate correlations are shown by the *R* values of 0.446 for CTx (Figure 3D) and 0.310 for NTx/creatinine (Figure 3E).

**Other Biochemistry Parameters.** No meaningful effect of KRN23 treatment was observed on AUEC<sub>n</sub> for other PD variables (Figure 4): serum calcium (*R* = 0.238, Figure 4A),

PTH (*R* = 0.118, Figure 4B), fasting 2-hour calcium/creatinine ratio (*R* = 0.058, Figure 4C), or 24-hour urine calcium (*R* = 0.146, Figure 4D). There were also no meaningful PK/PD correlations observed for the following PD variables: serum 25(OH)D (*R* = 0.160), creatinine (*R* = 0.351), ionized calcium (*R* = 0.099); and calcium (*R* = 0.146), creatinine (*R* = 0.149), and calcium/creatinine ratio (*R* = 0.291) in 24-hour urine samples (Supplementary Figure S1).

**Table 2.** KRN23 Pharmacokinetic Parameters

Dosing Interval	1	2	3	4
Number of subjects	27	27	27	26
$T_{max,n}$ (days)	8.50 ± 2.90 (2.98, 14.9) 34	7.04 ± 1.71 (3.95, 11.9) 24	7.45 ± 3.83 (1.96, 19.9) 27	7.00 ± 3.22 (2.87–15.0) 46
$C_{max,n}$ (ng/mL)	386 ± 145 (193, 688) 38	947 ± 307 (356, 1710) 32	2490 ± 843 (421, 3950) 34	4750 ± 1800 (1030, 8110) 38
$C_{min,n}$ (ng/mL)	147 ± 53.4 (60.7, 253) 36	364 ± 130 (119, 662) 36	1080 ± 587 (104, 2560) 54	1470 ± 827 (166, 2890) 56
$AUC_n$ ( $\mu\text{g} \cdot \text{h/mL}$ )	174 ± 63 (71.6, 316) 36	430 ± 127 (156, 685) 30	1220 ± 432 (228, 2350) 35	2610 ± 974 (572, 4280) 37
Data from all 4 dosing intervals (n = 27)				
$AUC_{last}$ ( $\mu\text{g} \cdot \text{h/mL}$ )	$AUC_{inf}$ ( $\mu\text{g} \cdot \text{h/mL}$ )	CL/F (mL/h/kg)	V/F (mL/kg)	$t_{1/2}$ (days)
4340 ± 1320 (1340–6450) 30	5240 ± 1880 (1570, 8990) 36	0.186 ± 0.0780 (0.0835, 0.472) 42	98.3 ± 34.6 (51.2, 21.2) 35	16.4 ± 5.83 (5.58, 29.5) 35

Mean ± standard deviation (min, max) CV% is reported.

### Anti-KRN23-Antibodies

No positive anti-KRN23 antibodies were detected after KRN23 treatment in any subject from screening assay testing. Therefore, no further confirmative assay was needed.

### Baseline FGF23 and Serum Pi Response

No apparent correlation between overall serum area under the effect concentration–time curve ( $AUEC_{last}$ ) for serum Pi and baseline intact FGF23 levels was observed ( $R = 0.0943$ ).

## Discussion

KRN23 given subcutaneously in 4 increasing doses every 28 days to adults with XLH, increased  $T_{mP}$ , and serum Pi and  $1,25(\text{OH})_2\text{D}$  concentrations in a KRN23 PK-dependent manner. The PK exposure to KRN23, as measured by  $C_{max,n}$ ,  $C_{min,n}$ , and  $AUC_n$  values, increased in a dose-proportional manner. The V/F for a typical subject weighing 70 kg was estimated to be 6.9 L, which is slightly larger than the plasma volume ( $3\text{--}5\text{L}^{26}$ ). The mean  $t_{1/2}$  for KRN23 (16.4 days) after multiple-dose KRN23 administration was similar to the mean  $t_{1/2}$  (17.6, 15.1, 13.4, and 18.7 days) after single subcutaneous administration of KRN23 at doses of 0.1, 0.3, 0.6, and 1.0 mg/kg, respectively, indicating that elimination of KRN23 is not dose dependent. Mean  $T_{max}$

values were similar across the 4 dosing intervals and ranged from 7.0 to 8.5 days, indicating that rate of absorption of KRN23 after subcutaneous administration was consistent during every 28-day dosing regimen. Because of intra-subject dose escalation of KRN23 in this study and a mean KRN23  $t_{1/2}$  of 16.4 days, steady-state conditions were not reached for any dose between 0.1 and 1.0 mg/kg. Administration of a fixed KRN23 dose every 4 weeks for at least 5 times of the KRN23  $t_{1/2}$  (ie, approximately 82 days) would be necessary to reach KRN23 steady-state serum concentrations.

Unlike a standard multiple ascending-dose study design for a novel monoclonal antibody therapy (parallel-dose groups),<sup>27</sup> the present study employed an intradose-escalation scheme. The design was based on the practical reason that the prevalence of XLH is only 1:20 000.<sup>6</sup> For the intradose-escalation design, the dose–response relationship cannot be analyzed directly. We therefore used PK exposure ( $AUC_n$ ) and PD response ( $AUEC_n$ ) for the assessment of PK/PD relationships.

This study demonstrated that increases in  $T_{mP}/\text{GFR}$ , serum Pi, and serum  $1,25(\text{OH})_2\text{D}$  ( $AUEC_n$ ) were linearly correlated with increases in KRN23 PK exposure ( $AUC_n$ ) following multiple-dose administration of KRN23 in adults with XLH.  $T_{mP}/\text{GFR}$  and serum Pi concentrations reached maximum values as KRN23 concentrations at

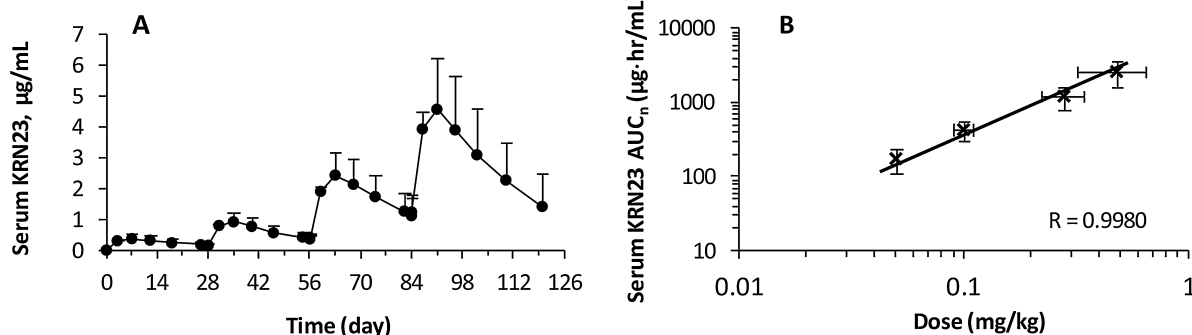


**Figure 1.** Mean serum KRN23 concentration over time (A) and dose proportionality between mean log KRN23  $AUC_n$  and mean log dose during the 4 dosing intervals (B). Error bars represent standard deviation (SD). The mean ± SD dose was  $0.05 \pm 0.0$ ,  $0.10 \pm 0.01$ ,  $0.28 \pm 0.06$ , and  $0.48 \pm 0.16$  mg/kg for dosing intervals 1, 2, 3, and 4, respectively.  $N = 27$  for dosing intervals 1 to 3 and  $n = 26$  for dosing interval 4.

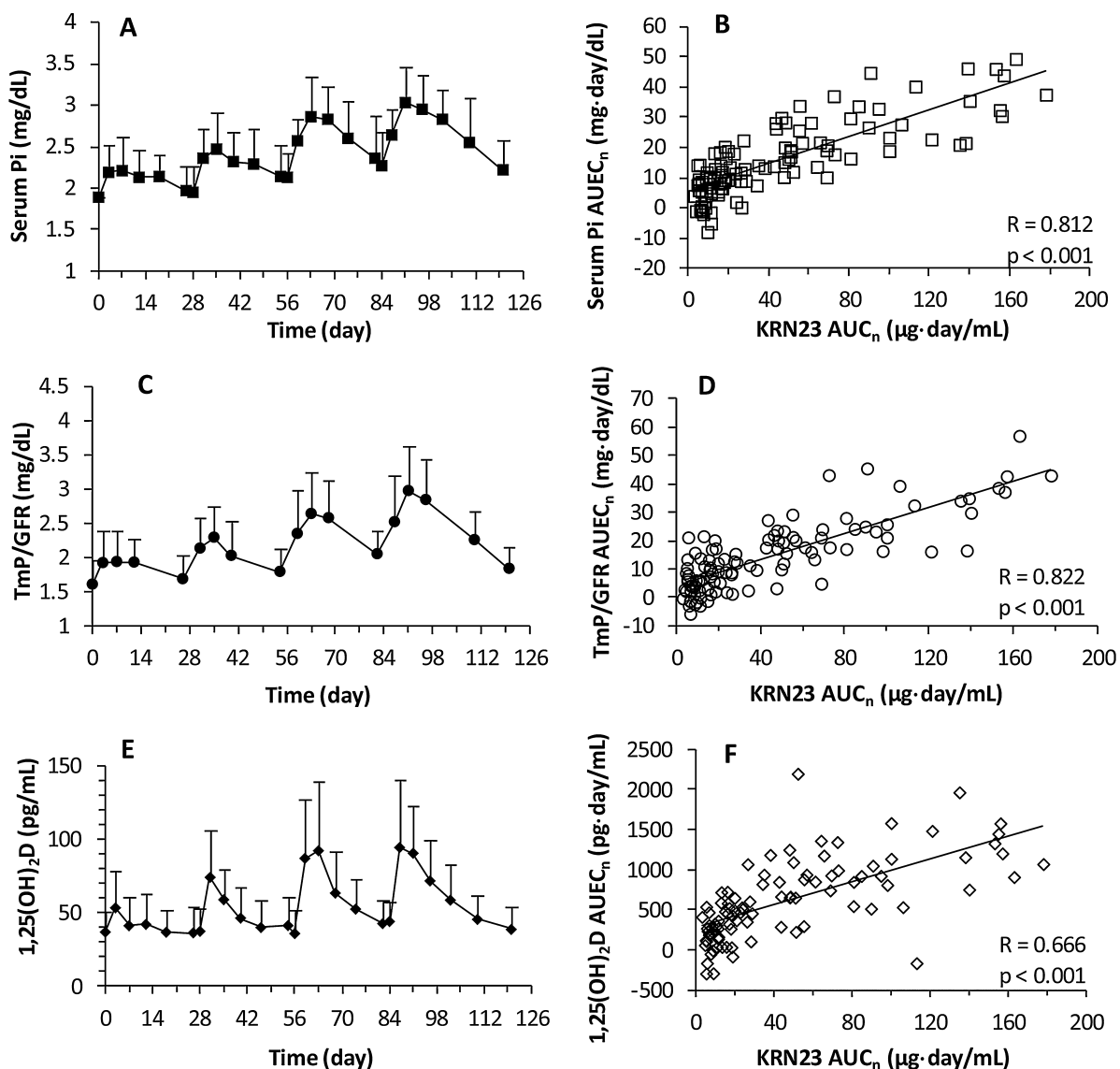


**Figure 2.** Pharmacodynamic (PD) profiles over 4 dosing intervals (left) and relationship of pharmacokinetic (PK) and PD parameters (right). (A and B) Serum Pi; (C and D) TmP/GFR; (E and F) 1,25(OH)<sub>2</sub>D. AUC<sub>n</sub>, area under the KRN23 serum concentration–time curve; AUEC<sub>n</sub>, area under the effect concentration–time curve for PD change from baseline during interval n (n = 1, 2, 3, or 4); R, Pearson correlation coefficient.

about the same time after each dose, and their levels increased and decreased in parallel. The direct relationship between serum KRN23 concentration and serum Pi increase reflects the dose-dependent blocking action of the antibody on renal phosphate reabsorption and supports dose adjustment of KRN23 based on peak and trough serum Pi concentrations.

In the present study, the body weight–based dose was employed instead of a fixed dose, which is usually used for subcutaneous route of administration.<sup>28</sup> As the study design was an intradose escalation, the body weight–based dosing strategy was employed to minimize variability.

In the present analysis, TmP/GFR values were both manually read using a nomogram<sup>24</sup> and calculated using

an equation.<sup>20</sup> The values derived from 2 methods resulted in a linear correlation with an *R* of 0.996. Thus, the equation<sup>20</sup> that is easier to perform than manual reading may be used in future clinical trials.

The increased serum 1,25(OH)<sub>2</sub>D levels observed in the study might have been expected to increase intestinal calcium absorption (not measured) and potentially increase serum calcium concentration and urine calcium excretion. However, serum calcium and urine calcium did not change, and there were no correlations between serum KRN23 concentrations and serum and urine calcium changes. This might suggest that the increased absorbed calcium was deposited in bone, a strong likelihood in the setting of osteomalacia in XLH patients.

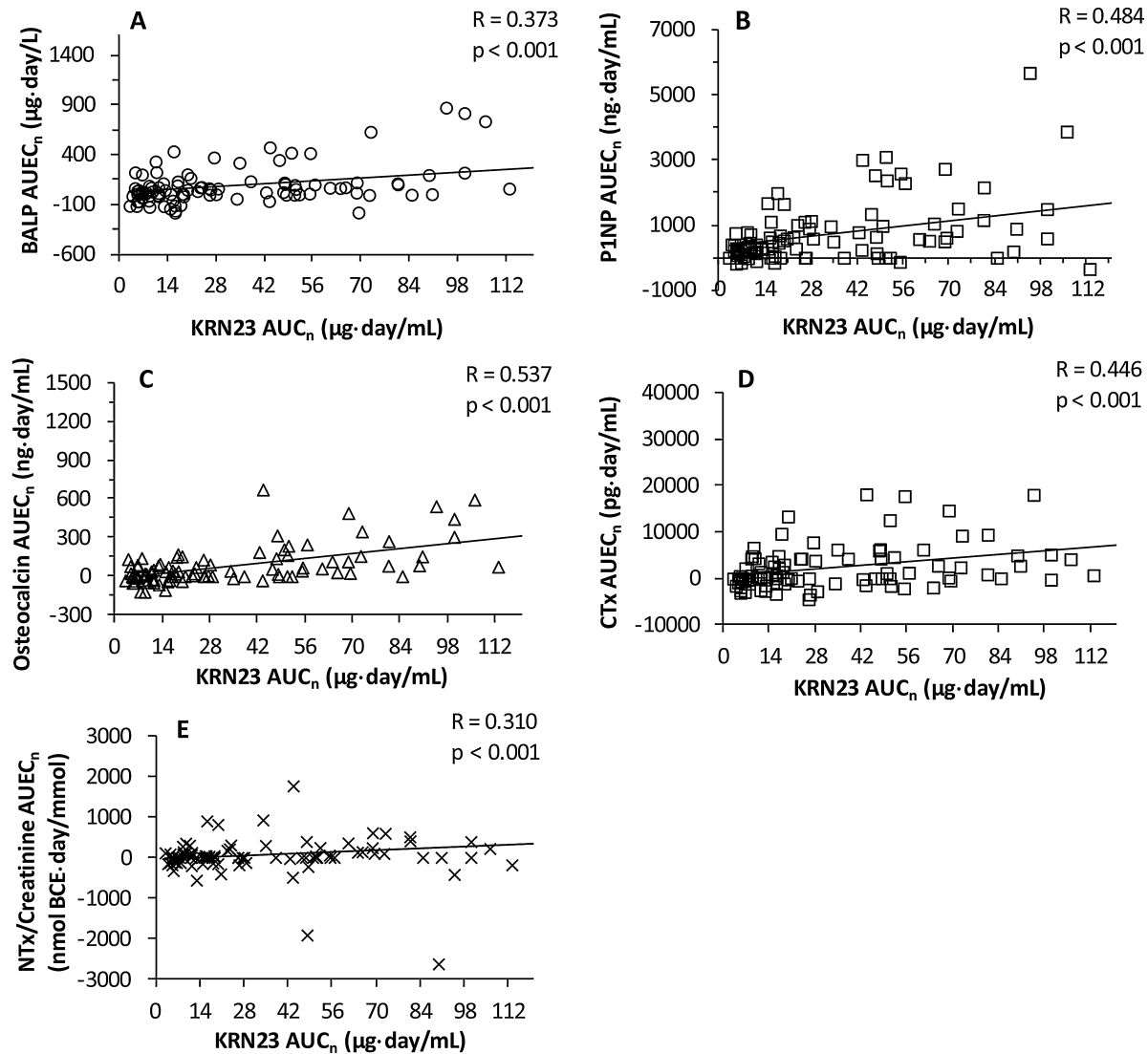


**Figure 3.** Relationship of pharmacokinetic and bone marker change from baseline. (A) BALP; (B) P1NP; (C) Osteocalcin; (D) CTx; (E) NTx/creatinine. AUC<sub>n</sub>, area under the KRN23 serum concentration–time curve; AUEC<sub>n</sub>, area under the effect concentration–time curve for bone marker change from baseline during interval n (n = 1, 2, 3, or 4); R, Pearson correlation coefficient.

The increases in serum 1,25(OH)<sub>2</sub>D may also have been expected to decrease the increased serum PTH levels resulting from secondary hyperparathyroidism present in many of the patients. However, no change in serum PTH was observed, possibly because resolution of secondary hyperparathyroidism takes considerably more time than that evaluated in this study.

The increase in both bone formation and bone resorption markers and the moderate correlation between their serum AUEC<sub>n</sub> and serum KRN23 AUC<sub>n</sub> is of great interest because it implies an indirect effect of KRN23 intervention on bone turnover. As a group, the patients had normal levels of bone biomarkers at baseline, although several subjects had clearly increased levels, probably indicating varying degrees of

osteomalacia. An initial paradoxical rise in both formation and resorption bone biomarkers was seen in patients with hypophosphatemic osteomalacia on starting treatment with the active vitamin D analogue, 1- $\alpha$  hydroxy vitamin D<sub>3</sub>, and phosphate supplements with the bone markers returning to normal reference range after several months of successful treatment.<sup>9</sup> The paradoxical initial increase is generally considered to be due to osteoblast stimulation of bone turnover. Thus, the rise in biomarkers with KRN23 suggests that the increase in serum phosphate and 1,25(OH)<sub>2</sub>D was starting to heal the osteomalacia.

Overall PK/PD results after multiple doses of KRN23 subcutaneous administration confirmed the PK/PD relationships observed after single-dose KRN23 subcutaneous



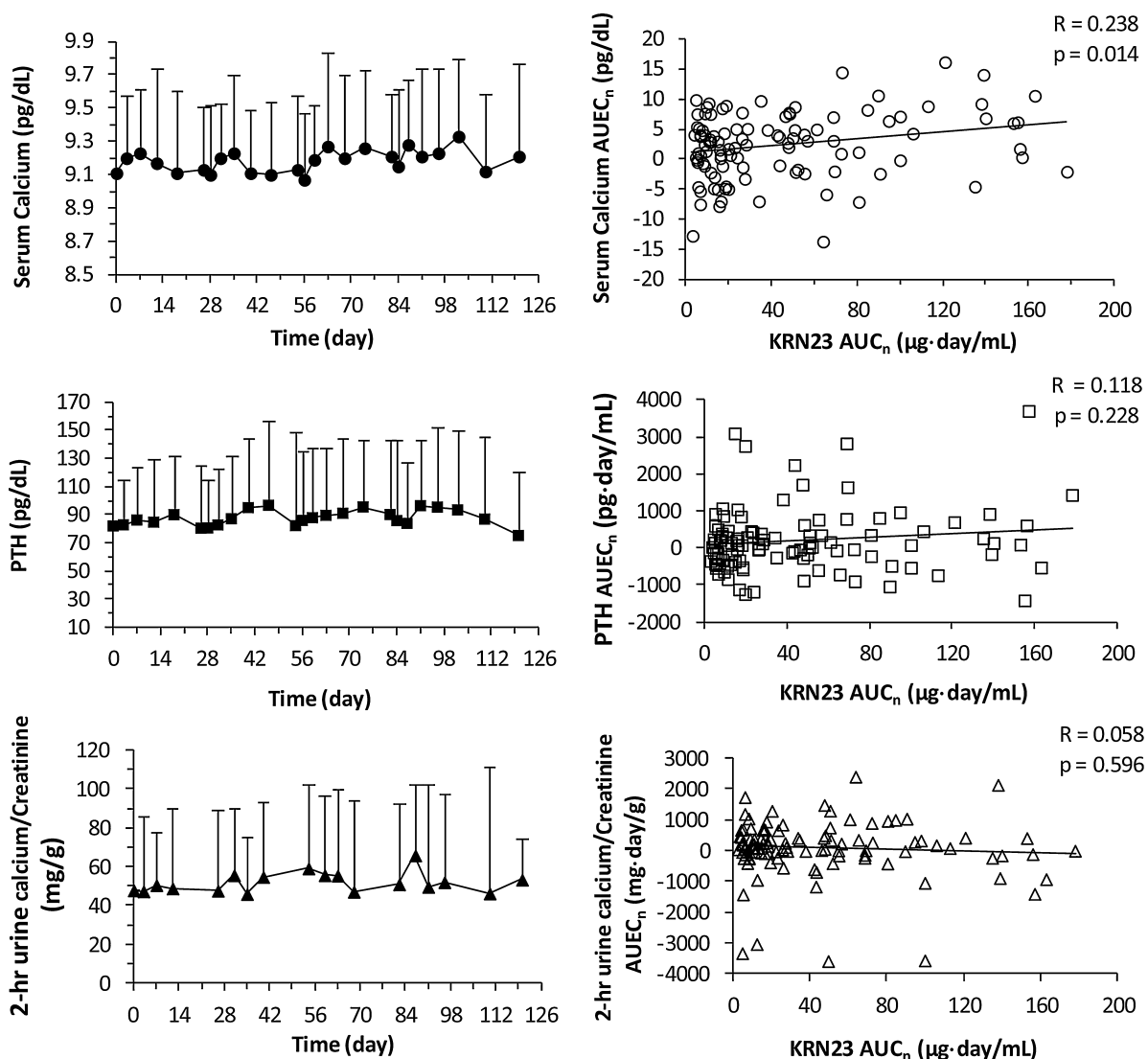


**Figure 4.** Pharmacodynamic (PD) profiles over 4 dosing intervals (left) and relationship of PK and PD parameters (right). (A and B) Serum calcium; (C and D) serum PTH; (E and F) 2-hour urine calcium/creatinine ratio; (G and H) 24-hour urine calcium. AUC<sub>n</sub>: area under the KRN23 serum concentration–time curve; AUEC<sub>n</sub>, area under the effect concentration–time curve for PD change from baseline during interval n (n = 1, 2, 3, or 4); R, Pearson correlation coefficient.

administration,<sup>15,16</sup> and further support the mechanism of action for KRN23 to block FGF23 activity.

In conclusion, the effects of KRN23 administered subcutaneously at 28-day intervals on serum Pi, TmP/GFR, and serum 1,25(OH)<sub>2</sub>D levels were sustained after each dose. There was also stimulation of bone turnover. PK dose proportionality and the linear PK/PD relationship between serum KRN23 and Pi concentrations support adjusting the KRN23 dose based on serum Pi levels. KRN23 is a promising treatment for XLH patients.

### Acknowledgments

We are grateful to the dedicated patients who participated in the study and to the subinvestigators, clinical study coordinators, and research nursing staff at the 6 study sites (Indiana University, Indianapolis, Indiana; The Methodist Hospital,

Houston, Texas; Duke University Medical Center, Durham, North Carolina; Shriners Hospital for Children, Montreal, Quebec, Canada; the University of California, San Francisco, San Francisco, California; and Yale University School of Medicine, New Haven, Connecticut). We thank Val Barra and Yamamoto Katsuhiko for analysis of serum KRN23 and FGF23 concentrations (Kyowa Hakko Kirin California, Inc, La Jolla, California), Kavita Gumbhir-Shah (PharmaMed Resources LLC, New Jersey) for conducting PK/PD data analysis, Shirley McKernan for editing and formatting of the manuscript (Kyowa Hakko Kirin Pharma, Inc.).

### Declaration of Conflicting Interests

The data in this article were obtained from the KRN23-INT-001 study funded by Kyowa Hakko Kirin Pharma Inc. Drs. T.O. Carpenter and M.D. Ruppe received consulting fees (other than

advisory board or board of directors) and research grants. Drs. Imel, Ruppe, Weber, Insogna, Portale, Glorieux, Peacock, and Carpenter received research grants during the study conduct. Drs. Zhang, Klausner, Vergeire, and Humphrey and Mr. Ito are employees of Kyowa Hakko Kirin Pharma Inc. Drs. E.A. Imel, T.O. Carpenter, M. Peacock, F.H. Glorieux, T.J. Weber, A.A. Portale, and K. Insogna have received research grants and/or consulting fees (other than advisory board or board of directors) from Ultragenyx Pharmaceuticals, Inc. for subsequent work related to KRN23.

## Funding

This study was funded by Kyowa Hakko Kirin Pharma Inc.

## References

- Imel EA, Econs MJ. Fibroblast growth factor 23: roles in health and disease. *J Am Soc Nephrol*. 2005;16:2565–2575.
- Liu S, Quarles LD. How fibroblast growth factor 23 works. *J Am Soc Nephrol*. 2007;18(6):1637–1647.
- Larsson T, Marshall R, Schipani E, et al. Transgenic mice expressing fibroblast growth factor 23 under the control of the alpha1(I) collagen promoter exhibit growth retardation, osteomalacia, and disturbed phosphate homeostasis. *Endocrinology*. 2004;145:3087–3094.
- Shimada T, Urakawa I, Yamazaki T, et al. FGF-23 transgenic mice demonstrate hypophosphatemic rickets with reduced expression of sodium phosphate cotransporter type IIa. *Biochem Biophys Res Commun*. 2004;314:409–414.
- Gattineni J, Bates C, Twombly K, et al. FGF23 decreases renal NaPi-2a and NaPi-2c expression and induces hypophosphatemia in vivo predominantly via FGF receptor 1. *Am J Physiol Renal Physiol*. 2009;297:F282–F291.
- Burnett CH, Dent CE, Harper C, Warland B. Vitamin D-resistant rickets. *Am J Med*. 1964;36:222–232.
- Tenenhouse HS, Econs NJ. Mendelian Hypophosphatemia. The Online Metabolic and Molecular Bases of Inherited Diseases (OMMBID); Part 21 (Chap. 197). [http://www.ommbid.com/OMMBID/the\\_online\\_metabolic\\_and\\_molecular\\_bases\\_of\\_inherited\\_disease/b/abstract/part21/ch197](http://www.ommbid.com/OMMBID/the_online_metabolic_and_molecular_bases_of_inherited_disease/b/abstract/part21/ch197). Accessed October 1, 2013.
- Reid IR, Hardy DC, Murphy WA, Teitelbaum SL, Bergfeld MA, Whyte MP. X-linked hypophosphatemia: a clinical, biochemical, and histopathologic assessment of morbidity in adults. *Medicine (Baltimore)*. 1989;68:336–352.
- Peacock M, Heyburn PJ, Aaron JE. Vitamin D resistant hypophosphatemic osteomalacia: treated with 1 alpha hydroxycalciferol D3. *Clin Endocrinol*. 1977;7:231S–237S.
- Glorieux FH, Marie PJ, Pettifor JM, Delvin EE. Bone response to phosphate salts, ergocalciferol, and calcitriol in hypophosphatemic vitamin D-resistant rickets. *N Eng J Med*. 1980;303:1023–1031.
- Harrell RM, Lyles KW, Harrelson JM, Friedman NE, Drezner MK. Healing of bone disease in X-linked hypophosphatemia rickets/osteomalacia. *J Clin Invest*. 1985;75:1858–1868.
- Costa T, Marie PJ, Scriver CR, et al. X-linked hypophosphatemia: effect of calcitriol on renal handling of phosphate, serum phosphate, and bone mineralization. *J Clin Endocrinol Metab*. 1981;52:463–472.
- Yamazaki Y, Tamada T, Kasai N, et al. Anti-FGF23 neutralizing antibodies show the physiological role and structural features of FGF23. *J Bone Miner Res*. 2008;23:1509–1518.
- Carpenter T, Imel EA, Holm IA, Jan de Beur SM, Insogna KL. A clinician's guide to X-linked hypophosphatemia. *J Bone Miner Res*. 2011;26(7):1381–1388.
- Aono Y, Yamazaki Y, Yasutake J, et al. Therapeutic effects of anti-FGF23 antibodies in hypophosphatemic rickets/osteomalacia. *J Bone Miner Res*. 2009;24:1879–1888.
- Carpenter T, Imel E, Ruppe M, et al. Randomized trial of the anti-FGF23 antibody KRN23 in X-linked hypophosphatemia. *J Clin Invest*. 2014;124:1587–1597.
- Zhang X, Carpenter T, Imel E, et al. Pharmacokinetics and pharmacodynamics of a human monoclonal anti-FGF23 antibody (KRN23) after single-dose administration to patients with X-linked hypophosphatemia. *J Bone Miner Res*. 2013;28(Suppl 1). <http://www.asbmr.org/asbmr-2013-abstract-detail?aid=0ee3ad49-1a6e-4a1e-bb65-4ceflcc43a02>. Accessed October 31, 2013.
- Imel EA, Zhang X, Ruppe MD, et al. The First Multi-Dose Trial of a Human Anti-FGF23 (Fibroblast Growth Factor 23) Antibody (KRN23) in Adults with X-Linked Hypophosphatemia (XLH). Oral presentation (OR43-1). 2014 ICE/ENDO Annual Meeting. June 21–24, 2014. Chicago, Illinois.
- Endo I, Fukumoto S, Keiichi O, et al. Clinical usefulness of measurement of fibroblast growth factor 23 (FGF23) in hypophosphatemic patients: Proposal of diagnostic criteria using FGF23 measurement. *Bone*. 2008;42(6):1235–1239.
- Payne RB. Renal tubular reabsorption of phosphate (TmP/GFR): indications and interpretation. *Ann Clin Biochem*. 1998;35:201–206.
- Gibaldi M, Perrier D. Non-compartmental analysis based on statistical moment theory. In: *Pharmacokinetics (Drugs and the Pharmaceutical Sciences)*. 2nd ed. New York, New York: Marcel Dekker Inc.; 1982 409–417.
- Yamazaki Y, Okazaki R, Shibata M, et al. Increased circulatory level of biologically active full-length FGF-23 in subjects with hypophosphatemic rickets/osteomalacia. *J Clin Endocrinol Metab*. 2002;87(11):4957–4960.
- Investigator Laboratory Instruction Manual. Quest Diagnostics Clinical Trials. Valencia, California.
- Walton RJ, Bijvoet OLM. Nomogram for derivation of renal threshold phosphate concentration. *Lancet*. 1975;309–310.
- Investigator Laboratory Instruction Manual. Esoterix Clinical Trials Services. A division of LabCorp. Cranford, New Jersey.
- Leveque D, Wisniewski S, Jehl F. Pharmacokinetics of therapeutic monoclonal antibodies used in oncology. *Anticancer Res*. 2005;25:2327–2344.
- Salloway S, Sperling R, Gilman S, et al. A phase 2 multiple ascending dose trial of bapineuzumab in mild to moderate Alzheimer disease. *Neurology*. 2009;73(24):2061–2070.
- Kavanaugh A, McInnes I, Mease P, et al. Golimumab, a new human tumor necrosis factor  $\alpha$  antibody, administered every four weeks as a subcutaneous injection in psoriatic arthritis: twenty-four-week efficacy and safety results of a randomized, placebo-controlled study. *Arthritis Rheum*. 2009;60(4):976–986.

## Supporting Information

Additional supporting information may be found in the online version of this article at the publisher's web-site.